Running head: Oxygen isotope variations in Scots pine

How does varying water supply affect oxygen isotope variations in needles and tree rings of Scots pine?

Galina Timofeeva[1,2,3], Kerstin Treydte[2], Harald Bugmann[3], Yann Salmon[4,5], Andreas Rigling[2], Marcus Schaub[2], Pierre Vollenweider[2], Rolf Siegwolf[1,2] and Matthias Saurer[1,2]

[1]Laboratory of Atmospheric Chemistry, Paul Scherrer Institute (PSI), Villigen 5232, Switzerland
[2]Research Unit Forest Dynamics, Swiss Federal Institute for Forest, Snow and Landscape Research WSL, Birmensdorf 8903, Switzerland
[3]Institute of Terrestrial Ecosystems, ETH Zurich, Zurich 8092, Switzerland
[4]Department of Physics, University of Helsinki, Helsinki 00014, Finland
[5]School of GeoSciences, University of Edinburgh, EH9 3FF Edinburgh, UK

* Corresponding author: matthias.saurer@wsl.ch, tel. +41-44-7392198

Accepted in Tree Physiology

Keywords:

Stable isotopes, climate change, tree mortality, *Pinus sylvestris*, post-photosynthetic fractionation

Abstract

In many regions, drought is suspected to be a cause of Scots pine decline and mortality, but the underlying physiological mechanisms remain unclear. Because of their relationship to ecohydrological processes, $\delta^{18}O$ values in tree rings are potentially useful for deciphering long-term physiological responses and tree adaptation to increasing drought. We therefore analysed both needle- and stem-level isotope fractionations in mature trees exposed to varying water supply. In a first experiment, we investigated seasonal $\delta^{18}O$ variations in soil and needle water of Scots pine in a dry inner-Alpine valley in Switzerland, comparing drought-stressed trees with trees that were irrigated for more than 10 years. In a second experiment, we analysed 20th century $\delta^{18}O$ variations in tree rings of the same forest, including a group of trees that had recently died. We observed less ^{18}O enrichment in needle water of drought-stressed compared to irrigated trees. We applied different isotope fractionation models to explain these results, including the Péclet- and the two-pool correction which considers the ratio of unenriched xylem water in the needles to total needle water. Based on anatomical measurements, we found this ratio to be unchanged in drought-stressed needles, although they were shorter. The observed lower ^{18}O enrichment in needles of stressed trees was therefore likely caused by increased effective path length for water movement within the leaf lamina. In the tree-ring study, we observed lower $\delta^{18}O$ values in tree rings of dead trees compared to survivors during several decades prior to their death. These lower values in declining trees are consistent with the lower needle water ^{18}O enrichment observed for drought-stressed compared to irrigated trees, suggesting this needle-level signal to be reflected in the tree-rings, although changes in rooting depth could also play a role. Our study demonstrates that long-term effects of drought are reflected in the tree-ring $\delta^{18}O$ values, which helps providing a better understanding of past tree physiological changes of Scots pine.

Introduction

Water is a key factor for plant growth and survival, and hence, understanding the variability in plant water uptake and transpiration is of paramount importance. This becomes even more pertinent in regions where plants experience acute or chronic drought that may lead to tree mortality (Allen et al. 2015; Allen et al. 2010; Anderegg et al. 2013; Choat et al. 2012). Understanding plant and particularly tree response to drought is a pressing issue in view of climate change, having triggered many studies (Breshears et al. 2013; McDowell et al. 2008). However, most experimental studies were performed with seedlings and saplings of various tree species (Cocozza et al. 2016; Duan et al. 2015; Galle et al. 2010; Pearson et al. 2013), and only rarely with mature trees (Aguadé et al. 2015; Galiano et al. 2010; Gaylord et al. 2015; Poyatos et al. 2013; Salmon et al. 2015). Therefore, drought manipulation studies in natural environments are crucial to further develop our understanding of the physiological responses of mature trees to drought, including associated isotope fractionations (Grossiord et al. 2018; Herzog et al. 2014; Rowland et al. 2015).

Stable oxygen isotope ratios (expressed as $\delta^{18}O$ values) in plant organic matter have already been used to investigate ecophysiological and ecohydrological responses during drought (Moreno-Gutiérrez et al. 2012; Sargeant and Singer 2016). It is known that $\delta^{18}O$ values of meteoric water are variable due to large-scale hydrological processes and temperature effects (Craig and Gordon 1965; Dansgaard 1964). These variations are reflected in soil water, with modification through mixing and evaporation. The soil water is taken up by plant roots without fractionation (Ehleringer and Dawson 1992), but in the leaves the isotope ratio is further changed owing to equilibrium and kinetic fractionation processes during transpiration (Dongmann et al. 1974; Farquhar et al. 2007) and carbohydrate production (Lehmann et al. 2017; Roden and Ehleringer 1999). Therefore, $\delta^{18}O$ variations in plant organic matter such as tree rings are characterized by a complex, mixed isotope signal arising from the source water, the evaporative leaf water ^{18}O enrichment, and biochemical source-to-sink isotope fractionations (Gessler et al. 2014).

Although $\delta^{18}O$ values in tree rings have often been used to reconstruct past environmental conditions (Edwards et al. 2008; Labuhn et al. 2016; Libby et al. 1976; Masson-Delmotte et al. 2005; Rinne et al. 2013; Treydte et al. 2006), these studies mainly relied on statistical relationships with climate variables and thus may not always adequately account for all

processes (McCarroll and Loader 2004; Treydte et al. 2014). It would be important to apply mechanistic, process-based models for better understanding the factors controlling the isotope fractionation in foliage and tree rings related to various environmental conditions, including drought. The mechanistic Craig-Gordon model has often been applied to this end, mostly at the leaf-level (Craig and Gordon 1965; Farquhar and Lloyd 1993). It has been critically discussed that this model often overestimates leaf water ^{18}O enrichment and thus needs a correction for improved accuracy (Barbour 2007; Ogée et al. 2007). To date, there is no general correction approach suitable across different species. In many studies, the so-called Péclet correction was applied, requiring sometimes rather unrealistic adjustments of its parameters (Cernusak et al. 2016; Ferrio et al. 2012; Song et al. 2013). Therefore, it has been suggested that the so-called two-pool correction could be more adequate, particularly for conifers (Bögelein et al. 2017; Roden et al. 2015; Song et al. 2015) or a combination of the two-pool model and Péclet correction (Holloway-Phillips et al. 2016). Additionally, current mechanistic models have been challenged by the limited understanding of post-photosynthetic isotope fractionation and the biochemical processes responsible for the incorporation of the cellulose oxygen isotopic signature into tree rings (Cheesman and Cernusak 2017; Gessler et al. 2009; Gessler et al. 2014; Ogée et al. 2009; Sternberg 2009; Waterhouse et al. 2002). During drought, various changes act in combination, such as temperature, source water composition, vapour pressure deficit, stomatal conductance and needle morphological properties. Therefore, it remains difficult to disentangle these factors and use $\delta^{18}O$ in tree rings as a proxy for reconstructing long-term environmental changes or for better understanding causes of tree mortality.

In this study, we investigated a drought-stressed Scots pine population from one of the driest parts of the European Alps (Valais, Switzerland) that has been subjected to a long-term irrigation experiment since 2003. In a first experiment, we measured $\delta^{18}O$ values in water extracted from different soil depths and needles of drought-stressed and irrigated trees sampled multiple times between 2013 and 2015. In a second experiment at the same site, we analyzed the $\delta^{18}O$ values in tree-ring cellulose from Scots pine trees that had recently died and compared them with the signal from living trees over the period 1900-2014. Our first aim was to identify the factors controlling leaf-level isotope fractionation of Scots pine under drought and irrigation, considering evaporative leaf water enrichment, gas-exchange and needle morphological properties. Particularly, the basic Craig-Gordon

model, Péclet and the two-pool correction were explored. Our second aim was to disentangle the effects of climate and tree physiology on long-term variations in $\delta^{18}O$ by comparing measured tree-ring $\delta^{18}O$ values with predicted ones using a fractionation model corrected with a similar approach as for needles. This should help to determine the driving factors of tree-ring oxygen isotope variability in drought-stressed Scots pine trees.

Materials and methods

Study site

The study was carried out in the Pfynwald forest (46º 18' N, 7º 36' E, 615 m a.s.l.) in Valais, Switzerland. The site is a natural Scots pine (*Pinus sylvestris* L.) forest located in one of the driest inner-Alpine valleys of the European Alps, where severe Scots pine decline and mortality have already been observed (Bigler et al. 2006; Rigling et al. 2013). The forest is characterized as uneven-aged Erico-Pinetum sylvestris with shallow soil and low water retention (Dobbertin et al. 2010). Because of the blockage of moist incoming oceanic air masses by the high surrounding mountain ranges, the climate in Central Valais is continental. For the 1981-2010 period, mean annual precipitation was 605 mm, with 169 mm only during summer, while the mean annual temperature was 10.1 °C (19.1 °C for summer). In 2003, an irrigation experiment was initiated at this site (Dobbertin et al. 2010; Eilmann et al. 2010; Herzog et al. 2014), consisting of four drought-stressed and four irrigated plots of 1000 m^2 each. The irrigation water was taken from a river channel near the experimental area, and irrigation took place every growing season between April and October. The irrigated trees received ca. twice the amount of total annual precipitation compared to the drought-stressed trees, i.e. approximately 1300 mm.

Sampling, sample preparation and measurements

To measure seasonal $\delta^{18}O$ variations in needle water, one tree per plot (i.e. four drought-stressed trees and four irrigated trees) was selected for repeated samplings between August 2013 and August 2015. Sampling was conducted every month from June to August and ca. every second month for the other periods. Several twigs were cut at a height of 10-12 m from the sun-exposed part of the crown using a pole pruner. Current-year needles were immediately separated from twigs, stored in air-tight glass vials with screw caps and placed in the dark in a cooling box with ice packs to minimize evaporative water loss.

At the same sampling dates, soil samples from each plot (4 per treatment) were collected at two depths (0-10 and 10-20 cm) and stored in air-tight glass vials to monitor seasonal $\delta^{18}O$ variations of the soil water. Deeper sampling depths were generally not accessible due to the rocky soil. However, there was one soil profile down to 80 cm available, where soil samples were excavated on April 9th, 2014. Water samples from the channel (irrigation source) were collected at each sampling date as well. Increment cores from the four drought-stressed and four irrigated trees were sampled for stem water extraction in August and October 2014 (one 0.5 cm core per tree). Because xylem water was not systematically collected during the experiment in 2013-2015, twig phloem, twig xylem and stem xylem samples during August 2017 were taken to confirm the difference in source water between drought-stressed and irrigated trees.

Water from soil, needles and tree increment cores was obtained using a cryogenic vacuum extraction system (Saurer et al. 2016; West et al. 2006). In brief, glass vials with samples were placed in a water bath at 80 ºC. The evaporated water from samples was collected into U-shaped glass tubes that were cooled down with liquid nitrogen. Both glass vials with samples and tubes were connected to a vacuum system at ca. 4×10^{-2} mbar. Subsequently, the extracted water samples were transferred into 2 ml sealed glass vials. The $\delta^{18}O$ values of these water samples were measured by injecting 0.6 µl of the sample into a Thermal Conversion Elemental Analyzer (TC/EA; Thermo Finnigan, Bremen, Germany), where the water was pyrolysed in a glassy carbon reactor at 1450 ºC to hydrogen (H_2) and carbon monoxide (CO). These gases were carried in a helium stream to an isotope ratio mass spectrometer (IRMS) Delta plus XP (Thermo Finnigan, Bremen, Germany) for $\delta^{18}O$ analysis. The results were reported in the standard δ-notation as per mil (‰) relative to the Vienna Standard Mean Ocean Water (VSMOW), with a precision of < 0.2 ‰.

Twelve stem disks of standing dead trees (subsequently called “now-dead/dead trees”) and increment cores from 32 trees (“now-living/living trees”) were sampled within the non-irrigated (drought-stressed/ambient) area. Tree-ring widths (TRW) were measured at the tree-ring laboratory of the Swiss Federal Institute for Forest, Snow and Landscape Research WSL in Birmensdorf, Switzerland. The chronologies of the dead and living trees cover the period of 1900-2005 and 1900-2014, respectively. For details on sampling, sample preparation and TRW measurements see Timofeeva *et al.* (2017). For $\delta^{18}O$ meas-

urements, the tree-rings were separated according to calendar year and cellulose was extracted following Leavitt and Danzer (1993) and Boettger et al. (2007), with modifications according to Roden et al. (2009), and homogenized with an ultra-sonic device (Laumer et al. 2009). *Aliquots* were packed into silver capsules for isotope analyses, which were conducted using a pyrolysis method at 1420 °C in an elemental analyzer (PYRO-cube, Elementar, Hanau, Germany) connected to an Isotope Ratio Mass Spectrometer (IRMS, Delta Plus XP) via a Conflo III interface (Thermo Fischer Scientific, Bremen, Germany) (Weigt et al. 2015). In general, the measurement precision was better than 0.2 ‰.

Needle gas exchange and anatomical measurements

Leaf gas exchange, including net photosynthesis (A_N) and transpiration (E) of five sun-exposed twigs per tree (4 irrigated trees, 4 drought-stressed trees) were measured in June 2013 and May and June 2014. Measurements were performed using a portable photosynthesis system equipped with a 6400-22L leaf chamber (LI-COR 6400Xt; LI-COR, Lincoln, NE, USA). Conditions in the cuvette were kept constant during the measurements at 400 ppm [CO_2] and a photon flux density of 1,000 μmol m^{-2} s^{-1}, while the temperature was adjusted close to ambient conditions. Initial leaf-gas exchange values were corrected *a posteriori* for the exact projected leaf area according to Fleck *et al.* (2016).

To measure the needle length of current-year needles, 10 trees at the drought-stressed and 12 trees at the irrigated plots were selected. Measurements were repeated every year during summer from 2013 to 2015. For the anatomical assessments of needles, one branch from the sun crown of 5 trees per experimental plot was pole-pruned in February 2015. Needle samples from the last three needle generations were fixed in 2.5 % glutaraldehyde buffered at pH 7.0 with a 0.067 M Soerensen phosphate buffer and stored at 4°C until processing (here, we only present data for the 2013 and 2014 needle generations). The size of tissues and histological composition were assessed using 70 µm hand-microtomed cross-sections from the hydrated middle-part of needles. The cuttings were visually analysed with bright field microscopy using the 10x objective of a Leica microscope Leitz DMRB and imaged using the Lumenera INFINITY 2.1R camera and Lumenera Infinity Analyze (release 6.4) software (Lumenera Corp., Ottawa, Canada). The total area of needle cross-sections and that of each tissue (epidermis; hypodermis; resin ducts; mesophyll;

endodermis; transfusion tissues; phloem; xylem) was determined by means of image analysis and the measurement tools in the Adobe Photoshop software (Cs5, version 12.0.0.0, Adobe Systems Inc., San Jose, CA, USA), using stitched micrographs. The histological composition was calculated by expressing each tissue in percentage area of the whole needle section.

Oxygen isotope modelling

As a first approximation, the needle water isotope ratio ($\delta^{18}O_N$) in the steady-state can be calculated by the Craig & Gordon (1965) equation modified by Dongmann *et al*. (1974):

$$\delta^{18}O_N = \delta^{18}O_{SW} + \varepsilon^+ + \varepsilon_k + (\delta^{18}O_V - \delta^{18}O_{SW} - \varepsilon_k)\cdot e_a/e_i, \quad (1)$$

where $\delta^{18}O_{SW}$ is the isotope value of the source water (xylem), ε^+ is the equilibrium fractionation related to the phase change from liquid to vapour, ε_k is the kinetic fractionation related to the diffusion in air, $\delta^{18}O_V$ is the atmospheric water vapour isotope value, and e_a/e_i is the ratio of leaf external (ambient) to internal water vapour pressures.

To exclusively characterize the isotope fractionation within the leaf without influences of the source water isotope variation, the leaf water enrichment term $\Delta^{18}O_N$ is often used, which is obtained after subtracting $\delta^{18}O_{SW}$ from $\delta^{18}O_N$:

$$\Delta^{18}O_N = \varepsilon^+ + \varepsilon_k + (\delta^{18}O_V - \delta^{18}O_{SW} - \varepsilon_k)\cdot e_a/e_i \quad (2)$$

We refer to this equation as the CG-model ("Craig-Gordon-model"). The equilibrium fractionation (ε^+) depends on temperature and can be calculated according to Bottinga & Craig, (1968):

$$\varepsilon^+ (‰) = 2.664 - 3.206\cdot10^3/\,T + 1.534\cdot10^6/\,T^2 \quad (3)$$

The kinetic fractionation (ε_k) has an approximate value of 28 ‰ (Cernusak et al. 2016). The e_a/e_i ratio can be simplified using relative air humidity (RH) for the calculations, assuming that RH inside the leaf is 100 % and that leaf and air temperatures are equal, although this may not always be the case, particularly for sun-exposed needles or leaves.

Parts of equations 1 and 2, i.e. $\delta^{18}O_V - \delta^{18}O_{SW}$, can be replaced by $-\varepsilon^+$, assuming isotopic equilibrium between soil (source) water and water vapour (Bögelein et al. 2017; Foerstel and Huetzen 1983).

Equations 1 and 2 were found to predict the variability of observed leaf water ^{18}O enrichment reasonably well (Cernusak et al. 2016; Farquhar and Lloyd 1993; Roden and Ehleringer 1999), but they often overestimate actual values. Therefore, a model correction based on the Péclet effect was proposed (Barbour 2007; Cernusak et al. 2016; Farquhar and Lloyd 1993). It can be characterized by the Péclet number $\wp$ and considers an isotopic gradient between xylem and evaporative sites, which is mainly driven by changes in transpiration (E) and the so-called effective path length (L):

$$\wp = L \cdot E/(C \cdot D) \quad (4)$$

where L (m) describes the tortuous path that water travels from the leaf veins to the sites of evaporation, E is the transpiration rate (mmol m^{-2} s^{-1}), C is the molar density of water (55.56×10^3 mol m^{-3}), and D is the diffusivity of $H_2{}^{18}O$ in water, which depends on temperature (Cernusak et al. 2016; Cuntz et al. 2007). However, the effective path length (L) is not a directly measurable parameter and difficult to quantify. Mostly, as in our study, it is determined by an iterative procedure to minimize the square-root of the sum of all differences between measured and modelled values (Barbour et al. 2004).

Leaf ^{18}O enrichment after the Péclet correction is then given as

$$\Delta^{18}O_N{}^* = \Delta^{18}O_N \cdot (1\text{-}e^{-\wp})/\wp \quad (5)$$

Furthermore, a two-pool model was suggested as a correction for the CG-model (Cernusak et al. 2016; Song et al. 2015; Yakir et al. 1990). It assumes that total needle water is a mixture of two discrete pools of water, i.e. unenriched water influenced mainly by xylem water (the central part of the needle consisting of endodermis, xylem, phloem, and transfusion tissues) and ^{18}O enriched water at the evaporative sites (mainly the mesophyll tissue), as follows:

$$\Delta^{18}O_N{}^* = \Delta^{18}O_N \cdot (1 - \varphi) \quad (6)$$

where φ is the ratio of unenriched to total needle water (Cernusak et al. 2016; Song et al. 2015) and can be experimentally determined from needle-anatomical measurements (Roden et al. 2015). This ratio φ can have a value between 0 (infinitely small xylem contribution) and 1 (xylem water fully dominates the $^{18}O/^{16}O$ ratio of needle water).

The two correction approaches can be combined, i.e. the Péclet correction is applied on the ^{18}O enriched part of the leaf water only (Holloway-Phillips et al. 2016):

$$\Delta^{18}O_N^* = (1 - \varphi)\Delta^{18}O_N \cdot (1\text{-}e^{-\wp})/\wp \quad (7)$$

A modified version of equation 1 can then be used to predict ^{18}O enrichment in tree rings:

$$\delta^{18}O_{TR} = \delta^{18}O_{SW} + (1\text{-}x) \cdot \Delta^{18}O_N^* + \varepsilon_{wc} \quad (8)$$

where $\delta^{18}O_{TR}$ is the predicted tree-ring isotope ratio, ε_{wc} is the biochemical exchange between the oxygen atoms of xylem water and those of the cellulose carbonyl groups, equaling 27 ‰ (DeNiro and Epstein 1981; Sternberg et al. 1986), and *x* is the proportion of oxygen atoms of carbonyl groups (e.g. of trioses) undergoing exchange with xylem (stem) water during cellulose formation (*x*=0.42). The value of x could vary as a function of the turnover of non-structural carbohydrates (Song et al. 2014) and environmental conditions (Cheesman and Cernusak 2017). This can also be expressed as a dampening *f* of the leaf water signal as reflected in the tree-ring $f = 1 - x = 0.58$ (Roden et al. 2000; Saurer et al. 1997; Treydte et al. 2014). As a surrogate for source water ($\delta^{18}O_{sw}$) variations over the investigated period, we used the averages of summer months of $\delta^{18}O$ in precipitation. The validity of this assumption was tested by comparison of measured soil $\delta^{18}O$-values with monthly $\delta^{18}O$ of precipitation (in Results). The needle water enrichment term $\Delta^{18}O_N^*$ in Eq. 8 can be expressed with the simple leaf CG-model (Eq. 2), resulting in what we subsequently call the "tree-ring CG-model", or using the more advanced expression from Eq. 7, resulting in the "full tree-ring model".

Climate data

For modeling of needle water ^{18}O enrichment, we used air temperature and relative humidity data from Pfynwald with 10 min resolution for the period of 2013-2015. These

data were obtained from Sensirion SHT-21 sensors with a multiple-plate radiation shield (±0.3 ºC and ±2% RH accuracy). Monthly climate data for 1900-2014 were obtained from the Sion meteorological station (MeteoSwiss archives). The Standardized Precipitation Evapotranspiration Index SPEI, a multiscalar drought index, was used for correlation analysis with tree-ring parameters (Timofeeva et al. 2017). Monthly $\delta^{18}O$ data of precipitation were obtained from the Global Network of Isotopes in Precipitation (GNIP) and from the Federal Office of Water and Geology, Bern, Switzerland (FOWG). The GNIP data from the Grimsel station (46.57 N, 8.33 E, 1950 m a.s.l.) for the period 1972-2014 were used for tree-ring $\delta^{18}O$ modeling. They were corrected for the elevational offset, using data from the Sion station for the period 1994-2014. To this end, we first calculated averages for each month for this period at both stations and used their differences for the correction. The raw data from the Sion station were not used for tree-ring modelling due to the short observation period.

Data analysis

We determined the response of $\delta^{18}O$ variations to climate by calculating Pearson's correlation coefficients between the monthly mean series of each climate variable (air temperature, precipitation, relative humidity, drought index and VPD) and $\delta^{18}O$ for individual months and seasons such as spring (March-May) and summer (June-August). We tested the significance of the correlation coefficients by applying two-tailed Student's t-tests. Temporal autocorrelation was taken into account by calculating the 'effective' sample size, which is based on sample size and the first-order autocorrelation for each time series and climate data:

$$N' = N \cdot \frac{(1 - r_1 \cdot r_2)}{(1 + r_1 \cdot r_2)} \quad (10)$$

where N is sample size; N' is effective sample size; and r_1 and r_2 are the first-order sample autocorrelation of the first and second time series, respectively (Dawdy 1964). Two-tailed Student's t-tests were applied to test for significant differences between groups. Two-factorial ANOVA was carried out to test for treatment and needle generation differences in needle anatomical data, including a Tukey's HSD Post-Hoc test.

Results

Seasonal variations in $\delta^{18}O$ of needle and soil water

The $\delta^{18}O$ values of needle water strongly fluctuated between sampling dates, showing seasonal differences with values up to ca. 10 ‰ during spring and summer, and negative values during winter (Fig 1a). Soil water $\delta^{18}O$ also featured a seasonal pattern at both measured soil depths, but with values always below zero (Fig. 1b,c). The $\delta^{18}O$ values of the channel water (source of irrigation) did not show significant seasonal changes and were depleted compared to soil water during the growing season (Fig. 1b,c; $p>0.05$). This depletion resulted in soil water $\delta^{18}O$ values of the irrigated plots to be clearly lower compared to the drought-stressed plots for both soil depths (significant for August 2013 and April 2014, $p < 0.05$). Isotope values at soil depths from 0 to 10 cm were generally enriched in ^{18}O compared to those at soil depths from 10 to 20 cm during spring and summer (except for summer 2014). This strong enrichment of water near the soil surface was consistent with the results of the deep soil profile taken on 09.04.2014 (Fig. S1). This profile showed that below a depth of 20 cm there was less variation in the isotopic composition. Furthermore, stem water collected in August and October 2014 showed $\delta^{18}O$ values close to soil water values from 20 cm depth rather than from top soil. Twig phloem, twig xylem and stem xylem samples taken after our experiment, while irrigation was still ongoing (August 2017), confirm the ^{18}O depletion of water taken up by irrigated trees compared to drought-stressed trees (Fig. S2). Considering all this information, the soil depth 10-20 cm was considered representative for the depth from where the source water was mainly taken up.

Needle water $\delta^{18}O$ values did not show any significant differences between drought-stressed and irrigated trees ($p>0.05$). However, it is important to consider that soil water $\delta^{18}O$ values of the irrigated plots were clearly lower compared to the drought-stressed plots due to lower $\delta^{18}O$ values in the channel water used for irrigation. Accordingly, calculated needle water enrichment above source water ($\Delta^{18}O$) based on the difference between $\delta^{18}O$ of needle water and water of soil depths 10-20 cm was higher for irrigated trees compared to the drought-stressed trees at almost all sampling points (Fig. 2). This divergence was most pronounced during spring and summer, although significant differences between drought-stressed and irrigated trees were only observed for August 2013 and April 2014 ($p < 0.05$), but not for the summer months of 2014 and 2015.

Gas exchange and needle properties

Transpiration rate per leaf area was on average higher for the irrigated compared to the drought-stressed trees, except for the sampling in June 2013 (Table 1). However, differences between treatments were only marginally significant ($p < 0.1$), whereas they were significant for the combined data of all tree in the treatment for both samplings in 2014 ($p < 0.01$) and for the combined sampling dates over the period of 2013-2014 ($p < 0.05$). These data were used to establish a linear relationship between E and VPD, which explained more than 60% of the variability in E and yielded a slope of 0.11 mmol m^{-2} sec^{-1} hPa^{-1} for drought-stressed and 0.19 mmol m^{-2} sec^{-1} hPa^{-1} for irrigated trees. This relationship was subsequently used to estimate E on dates without gas-exchange measurements needed for leaf water modeling.

Needles of the drought-stressed trees were shorter (on average 34.67 mm) compared to those of the irrigated trees (on average 44.31 mm), with a high variability for both treatments (Table 2). Differences in needle length between drought-stressed and irrigated trees were significant both for the averaged and for all measured values for 2013 ($p < 0.01$), 2014 ($p < 0.05$) and over the period of 2013-2014 ($p < 0.001$).

The cross-sectional area of the different needle tissues all showed a significant difference between the two needle generations (ANOVA, $p<0.01$; Table 3). Treatment (i.e. drought-stressed vs. irrigated) was significant for resin, transfusion tissues, phloem and xylem, while no interaction between needle generation and treatment was found. Differences in total needle cross-section between the drought-stressed and irrigated trees were not significant. We estimated the proportion of tissue not subjected to evaporative ^{18}O enrichment φ as the ratio of the sum of endodermis, xylem, phloem and transfusion tissues to total needle cross-section. This proportion amounted to 0.270±0.014 for drought-stressed and 0.282±0.013 for irrigated trees averaged over both needle generations. These values were used in the subsequent model calculations.

Modeling needle water ^{18}O enrichment

We found a highly significant correlation between measured and Craig-Gordon (CG)-modelled needle water ^{18}O enrichment values using the basic equation (Eq. 2, Fig. 3). However, modeled values were only accurate for winter conditions, when ^{18}O enrichment was low, but they were strongly overestimated for both treatments (by up to 10‰) during summer months (Fig. 3, Table 4). Accordingly, slopes of the linear regression strongly

deviated from 1 (Fig. 3a, *drought-stressed trees: slope = 0.44, R^2 = 0.66, p < 0.01; irrigated trees: slope = 0.53, R^2 = 0.62, p < 0.01*). Furthermore, the basic CG model could not explain the observed difference in ^{18}O enrichment between treatments. Results obtained from the model incorporating the Péclet- and two-pool corrections (Eq. 7) reflected the variability of the data much better, as the linear regression slopes were closer to 1 (Fig. 3b, *drought-stressed trees: slope = 0.88, R^2 = 0.67, p < 0.01; irrigated trees: slope = 0.83, R^2 = 0.64, p < 0.01*). Furthermore, average growing season values calculated with this model were very close to measured ^{18}O enrichment for both treatments and the difference between treatments of about 3.5 ‰ was well reproduced (Table 4). These calculations were based on φ derived from anatomical measurements and L optimized for minimum deviation from the data (Barbour et al. 2004). This resulted in high L of 0.32 m and 0.05 m for drought-stressed and irrigated groups, respectively. Even higher values of L of 0.7 m and 0.25 m would have resulted if neglecting the two-pool model (i.e. φ =0). Due to the high L, the Péclet effect (℘) was overall stronger for drought-stressed trees, despite the lower transpiration (Table 4), resulting in the lower ^{18}O enrichment observed compared to irrigated trees.

Tree-ring $\delta^{18}O$ values and their relationship to climate

The mean tree-ring $\delta^{18}O$ chronologies calculated from the five living and five now-dead trees, respectively, were highly correlated for the common period (Fig. 4a, 1900-2004, *r = 0.76, p < 0.001*), but also the mean inter-series correlations of the individual tree series for both groups where highly significant (Figs. S3 & S4). The tree-ring $\delta^{18}O$ chronologies of the living and the now-dead trees did not show any significant differences until the 1970s. After the 1970s, however, the records started to significantly deviate and remained lower for the now-dead trees until their death compared to the living trees (Fig. 4b, Student's t-test for differences between groups, 1900-1959: *0.130 ± 0.118 (mean difference ± SD), n.s.;* 1960-2005: *-0.786 ± 0.171, p < 0.001*). Correlation analysis between monthly climate variables and tree-ring $\delta^{18}O$ chronologies indicated the spring (Mar-May) and summer (Jun-Aug) seasons as most important for isotope fixation in the tree rings, and we thus focused on the correlations for these periods. Tree-ring $\delta^{18}O$ values of the living trees were positively and significantly correlated with spring temperatures and VPD (and negatively with RH), as well as with summer temperatures, precipitation amount and SPEI (Fig. 5). For the now-dead trees, correlations were similar and in some cases also

446 significant (spring VPD, summer precipitation amount and SPEI). Generally, trees that
447 died later showed a weaker response in spring, but a stronger response in summer com-
448 pared to living trees (Fig. 5).
449
450 *Modeling of $\delta^{18}O$ in tree rings*
451 Simulations of tree-ring $\delta^{18}O$ were performed for the time period where $\delta^{18}O$ data of pre-
452 cipitation are available (starting in 1972). We verified the representativeness of the pre-
453 cipitation $\delta^{18}O$ data as a surrogate for soil water isotopic composition by correlation anal-
454 ysis between measured seasonal soil water $\delta^{18}O$ of the study site (available 2013-2015)
455 and $\delta^{18}O$ of precipitation of various months. We found a highly significant correlation
456 between soil water values of 10-20 cm depth and 2-month precipitation averages (using
457 the current and the preceding month; $r^2 = 0.70$, $\delta^{18}O_{SW} = 0.8514*\delta^{18}O_{precipitation} + 1.679$).
458 This relationship was used to estimate the isotopic composition of soil water available for
459 the trees during the growing season over the extended period of 1972-2014. Other model
460 parameters were used as determined above for the drought-stressed trees, including the
461 relationship between E and VPD to estimate past variations in E.
462 The correlation between measured and modeled tree-ring $\delta^{18}O$ values was significant
463 when using the basic tree-ring CG-model (Eq. 8) for dying and surviving trees (*living*
464 *trees: slope = 0.31, R^2 = 0.33, $p < 0.001$; dead trees: slope = 0.32, R^2 = 0.38, $p < 0.001$*),
465 although the slopes deviated strongly from 1 and the estimated values were too high by
466 several per mil (Fig. 6). Applying the full model with the Péclet- and two-pool corrections
467 in Eq. 8, simulated values were in better agreement with measurements regarding both
468 the absolute level and the temporal variability (Fig. 6, *living trees: slope = 0.38, R^2 =*
469 *0.35, $p < 0.001$; dead trees: slope = 0.39, R^2 = 0.41, $p < 0.001$*). Using a range of values
470 for L, based on the value obtained from the first experiment for drought-stressed trees
471 (L=0.32 m ± 0.16m) shows the effect of this parameter on the tree-ring model results (Fig.
472 6). A higher L of 0.15 m for later dying trees compared to survivors would be consistent
473 with the observed average tree-ring $\delta^{18}O$ difference (0.79‰) between the two groups.
474 Furthermore, we attempted to explain remaining differences between modelled values for
475 this range of L and data by varying x in Eq. 8. Accordingly, we found a range of x= 0.24
476 to 0.37 for living trees, and a slightly higher range of x = 0.31 to 0.43 for dead trees.
477
478

Discussion

Comparison of measured and modelled needle water ^{18}O enrichment

In our first experiment on the seasonal variations in $\delta^{18}O$ of different water pools, the estimated ^{18}O enrichment using the CG model was too high for both drought-stressed and irrigated trees compared to observations of $\Delta^{18}O$, as often found in other studies (Cernusak et al. 2016), showing the need for a physiological correction. We also observed lower needle water ^{18}O enrichment for the drought-stressed compared to the irrigated trees that could not be explained by the basic CG-model, but by the full model considering the Péclet and two-pool corrections. The Péclet number $\wp$ is driven primarily by transpiration (E) and effective path length (L) and was shown to depend on water content and needle-anatomical traits (Liang et al. 2018). Under drought stress, transpiration often decreases due to lower stomatal conductance, as also observed at our site, which would reduce $\wp$ if L is unchanged (Eqs. 4, 5). Accordingly, needle water would be less diluted by re-filling with xylem water, and therefore higher needle $\Delta^{18}O$ values could be expected under drought stress, whereas an unconstrained water supply and low VPD would result in lower needle $\Delta^{18}O$ values. This was indeed observed in some studies (Roden and Ehleringer 1999; Yakir et al. 1990), but not in our case. However, $\wp$ depends also on the effective length of the water path within the leaf or needle, which can be affected by leaf/needle morpho-physiological changes under drought as well (Ferrio et al. 2012; Kahmen et al. 2008). Our results are therefore consistent assuming higher L for drought-stressed needles.

For deciduous plants, L can be estimated reasonably well (Kahmen et al. 2009), but for conifers, estimating L is often challenging, mostly due to the varying structure of a needle, its low conductance, and generally low transpiration. Very high estimates of more than one meter for L have previously been reported for various coniferous species, including pine (Song et al. 2013). Such values seem unrealistically high compared to the actual needle length, but could be related to the tortuosity of the water path and reduced hydraulic conductivity due to the xeromorphic structure of the needle. In gymnosperms, hydraulic connections between the xylem and the mesophyll are weak and the endodermis provides a hydraulic separation between the vascular strand and the rest of the needle (Zwieniecki et al. 2007).

By considering the two-pool model as in the full model, the Péclet correction is applied to the ^{18}O-enriched portion of needle water only and L is thus reduced (Holloway-Phillips et al. 2016). The two-pool model was originally proposed more than two decades ago (Gat and Bowser 1991; Yakir et al. 1990), but it has only recently been revived with the expectation that it may be superior to the Péclet model (Bögelein et al. 2017; Song et al. 2015). The advantage of the two-pool model is that its parameters are more easily accessible to direct observation. The model was found to explain well e.g. the different ^{18}O enrichment in old compared to young needles (Roden et al. 2015). When the proportion of the mesophyll tissue surrounding the needle xylem is relatively small (high φ value), the needle water signal will be strongly dominated by the unenriched xylem water, resulting in low $\Delta^{18}O$ according to the two-pool model. In our study, needle length of the drought-stressed trees was significantly lower than those of the irrigated ones. However, based on anatomical measurements, the calculated proportions of unenriched to enriched tissue did not change significantly (Table 3). This shows that needle shrinkage, i.e. the lower total cross-sectional area of the drought-stressed needles, was a result of smaller dimensions of all needle tissues. Our results and particularly the difference between irrigated and drought-stressed trees can therefore not be explained by the two-pool model alone, but its consideration is still important for proper application of the Péclet model.

One implicit assumption in the leaf models is the isotopic equilibrium between soil water and water vapour. This may not always be true, particularly under dry conditions, owing to soil evaporation effects (Bögelein et al. 2017; Ueta et al. 2013). There could also be a difference in relative humidity or $\delta^{18}O_v$ between drought-stressed and irrigated plots. We think, however, that such influence of added water to the soil is rapidly diluted in the air at 10-12 meters canopy height. Furthermore, it is crucial to use representative source water $\delta^{18}O$ values for modeling, particularly considering root distribution and isotopic gradients at different depths (Saurer et al. 2016; Treydte et al. 2014). Uncertainties regarding the soil depth from which trees take up water tend to be large. We used $\delta^{18}O$ values from the lower soil depth (10-20 cm), rather than values from the top layer, which were ^{18}O enriched due to evaporation from the soil surface. However, even when using the topsoil water values as the source, calculated needle water ^{18}O enrichment of the drought-stressed trees was still lower than the one of the irrigated trees. In addition, the $\delta^{18}O$ soil water values down to 80 cm determined from soil excavation did not show strong deviations

compared to those from 20 cm, suggesting that the source water values we used are likely to be appropriate.

Overall, the irrigation experiment enabled us to disentangle the effects of drought on needle-level oxygen isotope fractionation in mature trees, and we captured the important seasonal driving factors of needle water isotopic fractionation at our study site. This is an important prerequisite for understanding the tree-ring $\delta^{18}O$ values.

Tree-ring $\delta^{18}O$ variations in living and now-dead trees

The tree-ring $\delta^{18}O$ values of the individual living and now-dead trees as well as the means of the two groups featured very strong common variability (Figs. 4a, S3, S4). Our correlation analysis suggested that mainly spring mean temperature and VPD were responsible for the common $\delta^{18}O$ variations of both groups, consistent with earlier studies (Giuggiola et al. 2016; Treydte et al. 2014; Treydte et al. 2007). This can be explained by the effect of high temperatures on the isotope ratios of precipitation and source water (Dansgaard 1964), and by the higher foliar water ^{18}O enrichment under dry conditions (Roden and Ehleringer 1999), in general agreement with the factors known to influence oxygen isotope fractionations (Eq. 8). It is also consistent with the occurrence of frequent droughts in the studied region (Bigler et al. 2006; Rigling et al. 2013). However, dead trees were more depleted in $\delta^{18}O$ compared to the surviving trees after the 1970s (Fig. 4b). This indicates that climate alone cannot explain the isotope variability, but some site-specific soil or plant physiological differences must exist between the tree groups. The results from our seasonal water samples suggested that ^{18}O enrichment in drought-stressed trees was generally lower compared to the irrigated trees, owing to changes in needle morphology. This fits well to the lower tree-ring isotope values of the now-dead (i.e., more stressed) trees compared to the survivors. The lower needle water ^{18}O enrichment was related to higher effective path length L in drought-stressed trees and it could therefore be possible that such a signal is recorded in the tree-rings. This hypothesis will be further discussed in the modelling section below.

However, a direct mechanistic link between needle-level and stem-level signals is difficult to establish. Lower tree-ring $\delta^{18}O$ values in declining trees could also be related to seasonal differences in the use of carbohydrates (Sarris et al. 2013). Drought-stressed trees react more sensitively to favorable spring and early summer environmental conditions and therefore rely more on isotopically depleted source water from winter and

spring. Tree rings may therefore reflect the isotopic signature of carbohydrates produced during the earlier part of the growing season rather than during very dry conditions in summer (Pflug et al. 2015; Sarris et al. 2013). Furthermore, lower tree-ring $\delta^{18}O$ values in stressed trees may be related to different rooting patterns and associated changes in depth of the water source compared to more healthy trees (Brinkmann et al. 2019; Volkmann et al. 2016). However, this is unlikely at our site, as the lower values would imply deeper roots of the later dying trees. This would be unexpected for already weakened trees.

Long-term differences in gas-exchange between dying and surviving trees are indicated by a tree-ring study based on carbon isotopes at the same site (Timofeeva et al. 2017). The authors found that individuals with the most isohydric strategy were most prone to suffer as a result of long-term reduced carbon uptake (Timofeeva et al. 2017). As atmospheric moisture demand has been increasing during recent decades due to higher temperatures and more frequent drought (Rebetez and Dobbertin 2004), Scots pine trees tended to close their stomata and strongly reduced transpiration – potentially already for many decades at our study site. This does, however, not need to be the case on the verge of death, as dying Scots pines in Spain transpired even more than healthy individuals (Salmon et al. 2015). More insights into causes of the tree-ring isotope variations could be expected by the use of the isotope fractionation model.

Tree-ring isotope model

We applied isotope fractionation models only over the period where isotope data of precipitation were available (1972-2014). Nevertheless, the availability of such a long precipitation $\delta^{18}O$ record is precious and restricted to only a few sites globally. Modeling of $\delta^{18}O$ variations in tree-ring cellulose is more challenging (Roden et al. 2000; Saurer et al. 2012; Treydte et al. 2014) than modeling of changes in leaf/needle water $\delta^{18}O$ values (Barbour 2007; Cernusak et al. 2016). Besides the problem of the unknown source water isotope variability, including uncertainty about the seasonal distribution of precipitation in the soil, the transfer of the isotope signal from leaf water to organic compounds in leaves such as sucrose and later cellulose is complex and involves isotope fractionation at various steps (Gessler et al. 2014; Treydte et al. 2014). Fractionations may occur because of the use of stored carbohydrates or during phloem loading and transport, but the

609 strongest modifications are observed during cellulose formation due to exchange of car-
610 bonyl groups with xylem water, thus diluting the leaf isotope signal (Lehmann et al. 2017;
611 Sternberg et al. 1986). Therefore, previous studies faced challenges in extracting a leaf
612 physiological signal from tree-ring cellulose/wood $\delta^{18}O$ variations (Ogée et al. 2009;
613 Treydte et al. 2014).
614 In our study, tree-ring cellulose $\delta^{18}O$ values estimated with the basic CG model were too
615 high. However, applying the full model with an optimized Péclet path length (L) correc-
616 tion for each group of trees (Eq. 8) strongly improved the agreement between data and
617 model. The L values obtained were higher for the later dying trees (L = 0.48 m) compared
618 to surviving trees (L = 0.16 m), consistent with lower transpiration rates for the more
619 stressed trees. These values are in similar range as those obtained from modeling the sea-
620 sonal needle data (L = 0.32 m vs. 0.05 m). However, other model parameters could also
621 differ between the groups of trees, notably the proportion x of isotope exchange with
622 xylem water during cellulose formation (Cheesman and Cernusak 2017; Song et al. 2014).
623 In a study with eucalyptus trees in Australia, x was estimated to range from 0.21 to 0.68
624 and increase with increasing site aridity (Cheesman and Cernusak 2017). Based on a func-
625 tional link between x and the turnover of non-structural carbohydrates (Song et al. 2014),
626 this would suggest high cycling of triose phosphates in stem tissues in dry environments,
627 although in Song et al. (2014) the change of x with precipitation amount was not signifi-
628 cant. In our study, we find relatively low values, which are, however, not far from the
629 generally assumed x=0.42 for heterotrophic cellulose synthesis from sucrose. Values are
630 slightly higher for later dying, i.e. more stressed trees (0.31 to 0.43) compared to living
631 trees (0.24 to 0.37), which would be consistent with a higher turnover of non-structural
632 carbohydrates in stem tissues. This makes sense in a carbon-limited situation as a small
633 sucrose pool is turned over quickly during cellulose synthesis with less opportunity for
634 hexose phosphates to cycle through triose.
635

636 **Conclusions**

637 A combination of observed data and model simulations enabled us to derive valuable
638 information on past tree physiological changes at our site. Interestingly, lower $\delta^{18}O$ values
639 were also observed for declining Norway spruce (*Picea abies* L. Karst.) at two sites in
640 Norway (Hentschel et al. 2014). In this study, the authors concluded that such behavior

may be due to changes in anatomical and physiological traits of trees under drought conditions, which could be examined to infer the risk of future tree decline. Therefore, such changes and related isotope traces under drought could be common for conifers, and $\delta^{18}O$ may be helpful for estimating the 'health status' of trees, particularly in combination with $\delta^{13}C$ (Gessler et al. 2018; Scheidegger et al. 2000). Our results are among the first demonstrating needle-level changes in ^{18}O enrichment of trees exposed to long-term drought could be reflected in the $\delta^{18}O$-variations of tree rings. This method can potentially be applied either for retrospectively analyzing past tree-physiological changes, or even to predict decline and/or mortality of vulnerable trees.

Acknowledgments

We gratefully acknowledge the technical assistance by Magdalena Nötzli, Anne Verstege, Loic Schneider, Dieter Trummer, Walter Godli and Crest Simeon with wood sampling, preparation and measurements at ETH and WSL and by Theresia Lindner with the anatomical assessments at WSL. We also thank the technical coordinators of the Pfynwald Irrigation Experiment, Peter Bleuler and Christian Hug, for their support and Lola Schmid for stable isotope measurements. Furthermore, we thank Katja Rinne, Jan Blees, Rosemarie Barbara Weigt, Marco Lehmann, Lucia Galiano, Quim Canelles, Linda Feichtinger, as well as Konrad Egger and his team from Forstrevier Leuk for their assistance.

Funding

This study was financially supported by the Swiss State Secretariat for Education, Research and Innovation (SBFI) under COST Action FP1106 'STREeSS' (grant no. SBFC12.0093), SNF (No. 200020_182092 to M. Saurer; 200021_175888 to K. Treydte) and by NERC (RA0929 to M. Mencuccini) and the Academy of Finland (1284701 to T. Vesala).

References

Aguadé, D., R. Poyatos, T. Rosas and J. Martínez-Vilalta. 2015. Comparative drought responses of *Quercus ilex* L. and *Pinus sylvestris* L. In a montane forest undergoing a vegetation shift. Forests. 6:2505-2529.

Allen, C.D., D.D. Breshears and N.G. McDowell. 2015. On underestimation of global vulnerability to tree mortality and forest die-off from hotter drought in the Anthropocene. Ecosphere. 6:1-55.

Allen, C.D., A.K. Macalady, H. Chenchouni, D. Bachelet, N. McDowell, M. Vennetier, T. Kitzberger, A. Rigling, D.D. Breshears and E.T. Hogg. 2010. A global overview of drought and heat-

677 induced tree mortality reveals emerging climate change risks for forests. Forest Ecology
678 and Management. 259:660-684.
679 Anderegg, W.R.L., J.M. Kane and L.D.L. Anderegg. 2013. Consequences of widespread tree
680 mortality triggered by drought and temperature stress. Nature Clim. Change. 3:30-36.
681 Barbour, M.M. 2007. Stable oxygen isotope composition of plant tissue: a review. Functional
682 Plant Biology. 34:83-94.
683 Barbour, M.M., J.S. Roden, G.D. Farquhar and J.R. Ehleringer. 2004. Expressing leaf water and
684 cellulose oxygen isotope ratios as enrichment above source water reveals evidence of a
685 Peclet effect. Oecologia. 138:426-435.
686 Bigler, C., O.U. Bräker, H. Bugmann, M. Dobbertin and A. Rigling. 2006. Drought as an inciting
687 mortality factor in Scots pine stands of the Valais, Switzerland. Ecosystems. 9:330-343.
688 Boettger, T., M. Haupt, K. Knöller, S.M. Weise, J.S. Waterhouse, K.T. Rinne, N.J. Loader, E.
689 Sonninen, H. Jungner, V. Masson-Delmotte, M. Stievenard, M.-T. Guillemin, M. Pierre,
690 A. Pazdur, M. Leuenberger, M. Filot, M. Saurer, C.E. Reynolds, G. Helle and G.H. Schleser.
691 2007. Wood cellulose preparation methods and mass spectrometric analyses of $\delta^{13}C$,
692 $\delta^{18}O$, and nonexchangeable $\delta^{2}H$ values in cellulose, sugar, and starch: An
693 interlaboratory comparison. Analytical Chemistry. 79:4603-4612.
694 Bögelein, R., F.M. Thomas and A. Kahmen. 2017. Leaf water ^{18}O and ^{2}H enrichment along vertical
695 canopy profiles in a broadleaved and a conifer forest tree. Plant, Cell & Environment:doi:
696 10.1111/pce.12895.
697 Bottinga, Y. and H. Craig. 1968. Oxygen isotope fractionation between CO_2 and water, and the
698 isotopic composition of marine atmospheric CO_2. Earth and Planetary Science Letters.
699 5:285-295.
700 Breshears, D.D., H.D. Adams, D. Eamus, N.G. McDowell, D.J. Law, R.E. Will, A.P. Williams and C.B.
701 Zou. 2013. The critical amplifying role of increasing atmospheric moisture demand on
702 tree mortality and associated regional die-off. Frontiers in Plant Science. 4
703 Brinkmann, N., W. Eugster, N. Buchmann and A. Kahmen. 2019. Species-specific differences in
704 water uptake depth of mature temperate trees vary with water availability in the soil.
705 Plant Biology. 21:71-81.
706 Cernusak, L.A., M.M. Barbour, S.K. Arndt, A.W. Cheesman, N.B. English, T.S. Feild, B.R. Helliker,
707 M.M. Holloway-Phillips, J.A.M. Holtum, A. Kahmen, F.A. McInerney, N.C. Munksgaard,
708 K.A. Simonin, X. Song, H. Stuart-Williams, J.B. West and G.D. Farquhar. 2016. Stable
709 isotopes in leaf water of terrestrial plants. Plant, Cell & Environment. 39:1087-1102.
710 Cheesman, A.W. and L.A. Cernusak. 2017. Infidelity in the outback: climate signal recorded in
711 $\Delta^{18}O$ of leaf but not branch cellulose of eucalypts across an Australian aridity gradient.
712 Tree Physiology. 37:554-564.
713 Choat, B., S. Jansen, T.J. Brodribb, H. Cochard, S. Delzon, R. Bhaskar, S.J. Bucci, T.S. Feild, S.M.
714 Gleason, U.G. Hacke, A.L. Jacobsen, F. Lens, H. Maherali, J. Martinez-Vilalta, S. Mayr, M.
715 Mencuccini, P.J. Mitchell, A. Nardini, J. Pittermann, R.B. Pratt, J.S. Sperry, M. Westoby,
716 I.J. Wright and A.E. Zanne. 2012. Global convergence in the vulnerability of forests to
717 drought. Nature. 491:752-755.
718 Cocozza, C., M. de Miguel, E. Pšidová, L.u. Ditmarová, S. Marino, L. Maiuro, A. Alvino, T.
719 Czajkowski, A. Bolte and R. Tognetti. 2016. Variation in Ecophysiological Traits and
720 Drought Tolerance of Beech (*Fagus sylvatica* L.) Seedlings from Different Populations.
721 Frontiers in Plant Science. 7:886.
722 Craig, H. and L.I. Gordon. 1965. Deuterium and Oxygen 18 Variations in the Ocean and the
723 Marine Atmosphere. Consiglio nazionale delle richerche, Laboratorio de geologia
724 nucleare.
725 Cuntz, M., J. Ogée, G.D. Farquhar, P. Peylin and L.A. Cernusak. 2007. Modelling advection and
726 diffusion of water isotopologues in leaves. Plant, Cell & Environment. 30:892-909.
727 Dansgaard, W. 1964. Stable isotopes in precipitation. Tellus. 16:436-468.

728 Dawdy, D.R. 1964. Statistical and probability analysis of hydrologic data, part III: Analysis of
729 variance, covariance and time series, in Handbook of Applied Hydrology, edited by Ven
730 Te Chow. 868-890 p.
731 DeNiro, M.J. and S. Epstein. 1981. Isotopic composition of cellulose from aquatic organisms.
732 Geochimica et Cosmochimica Acta. 45:1885-1894.
733 Dobbertin, M., B. Eilmann, P. Bleuler, A. Giuggiola, E.G. Pannatier, W. Landolt, P. Schleppi and A.
734 Rigling. 2010. Effect of irrigation on needle morphology, shoot and stem growth in a
735 drought-exposed *Pinus sylvestris* forest. Tree Physiology. 30:346-360.
736 Dongmann, G., H.W. Nürnberg, H. Förstel and K. Wagener. 1974. On the enrichment of $H_2{}^{18}O$ in
737 the leaves of transpiring plants. Radiation and Environmental Biophysics. 11:41-52.
738 Duan, H., A.P. O'Grady, R.A. Duursma, B. Choat, G. Huang, R.A. Smith, Y. Jiang and D.T. Tissue.
739 2015. Drought responses of two gymnosperm species with contrasting stomatal
740 regulation strategies under elevated [CO_2] and temperature. Tree Physiology. 35:756-
741 770.
742 Edwards, T.W.D., S.J. Birks, B.H. Luckman and G.M. MacDonald. 2008. Climatic and hydrologic
743 variability during the past millennium in the eastern Rocky Mountains and northern
744 Great Plains of western Canada. Quaternary Research. 70:188-197.
745 Ehleringer, J.R. and T.E. Dawson. 1992. Water uptake by plants: perspectives from stable isotope
746 composition. Plant, Cell & Environment. 15:1073-1082.
747 Eilmann, B., N. Buchmann, R. Siegwolf, M. Saurer, P. Cherubini and A. Rigling. 2010. Fast
748 response of Scots pine to improved water availability reflected in tree-ring width and
749 $\delta^{13}C$. Plant, Cell & Environment. 33:1351-1360.
750 Farquhar, G.D., L.A. Cernusak and B. Barnes. 2007. Heavy water fractionation during
751 transpiration. Plant Physiol. 143:11-8.
752 Farquhar, G.D. and J. Lloyd. 1993. Carbon and Oxygen Isotope Effects in the Exchange of Carbon
753 Dioxide between Terrestrial Plants and the Atmosphere. *In* Stable Isotopes and Plant
754 Carbon-water Relations. Academic Press, San Diego, pp 47-70.
755 Ferrio, J.P., A. Pou, I. Florez-Sarasa, A. Gessler, N. Kodama, J. Flexas and M. Ribas-Carbó. 2012.
756 The Péclet effect on leaf water enrichment correlates with leaf hydraulic conductance
757 and mesophyll conductance for CO_2. Plant, Cell & Environment. 35:611-625.
758 Fleck, S., S. Raspe, M. Cater, P. Schleppi, L. Ukonmaanaho, M. Greve, C. Hertel, W. Weis, S.
759 Rumpf, A. Thimonier, F. Chianucci and P. Beckschäfer. 2016. Part XVII: Leaf Area
760 Measurements. In: UNECE ICP Forests Programme Co-ordinating Centre (ed.): Manual
761 on methods and criteria for harmonized sampling, assessment, monitoring and analysis
762 of the effects of air pollution on forests. Thünen Institute of Forest Ecosystems,
763 Eberswalde, Germany. 44 p. p.
764 Foerstel, H. and H. Huetzen. 1983. $^{18}O/^{16}O$ ratio of water in a local ecosystem as a basis of climate
765 record. IAEA, International Atomic Energy Agency (IAEA).
766 Galiano, L., J. Martínez-Vilalta and F. Lloret. 2010. Drought-Induced Multifactor Decline of Scots
767 Pine in the Pyrenees and Potential Vegetation Change by the Expansion of Co-occurring
768 Oak Species. Ecosystems. 13:978-991.
769 Galle, A., J. Esper, U. Feller, M. Ribas-Carbo and P. Fonti. 2010. Responses of wood anatomy and
770 carbon isotope composition of *Quercus pubescens* saplings subjected to two
771 consecutive years of summer drought. Annals of Forest Science. 67:809-809.
772 Gat, J.R. and C. Bowser. 1991. The heavy isotope enrichment of water in coupled evaporative
773 systems. *In* Stable Isotope Geochemistry: A Tribute to Samuel Epstein Eds. H.P. Taylor,
774 Jr., J.R. O'Neil and I.R. Kaplan.
775 Gaylord, M.L., T.E. Kolb and N.G. McDowell. 2015. Mechanisms of piñon pine mortality after
776 severe drought: a retrospective study of mature trees. Tree Physiology. 35:806-816.

Gessler, A., E. Brandes, N. Buchmann, G. Helle, H. Rennenberg and R.L. Barnard. 2009. Tracing carbon and oxygen isotope signals from newly assimilated sugars in the leaves to the tree-ring archive. Plant, Cell & Environment. 32:780-795.

Gessler, A., M. Cailleret, J. Joseph, L. Schonbeck, M. Schaub, M. Lehmann, K. Treydte, A. Rigling, G. Timofeeva and M. Saurer. 2018. Drought induced tree mortality - a tree-ring isotope based conceptual model to assess mechanisms and predispositions. New Phytologist. 219:485-490.

Gessler, A., J.P. Ferrio, R. Hommel, K. Treydte, R.A. Werner and R.K. Monson. 2014. Stable isotopes in tree rings: towards a mechanistic understanding of isotope fractionation and mixing processes from the leaves to the wood. Tree Physiology. 34:796-818.

Giuggiola, A., J. Ogée, A. Rigling, A. Gessler, H. Bugmann and K. Treydte. 2016. Improvement of water and light availability after thinning at a xeric site: which matters more? A dual isotope approach. New Phytologist. 210:108-121.

Grossiord, C., S. Sevanto, J.M. Limousin, P. Meir, M. Mencuccini, R.E. Pangle, W.T. Pockman, Y. Salmon, R. Zweifel and N.G. McDowell. 2018. Manipulative experiments demonstrate how long-term soil moisture changes alter controls of plant water use. Environmental and Experimental Botany. 152:19-27.

Hentschel, R., S. Rosner, Z.E. Kayler, K. Andreassen, I. Børja, S. Solberg, O.E. Tveito, E. Priesack and A. Gessler. 2014. Norway spruce physiological and anatomical predisposition to dieback. Forest Ecology and Management. 322:27-36.

Herzog, C., J. Steffen, E. Graf Pannatier, I. Hajdas and I. Brunner. 2014. Nine Years of Irrigation Cause Vegetation and Fine Root Shifts in a Water-Limited Pine Forest. PLoS ONE. 9:e96321.

Holloway-Phillips, M., L.A. Cernusak, M. Barbour, X. Song, A. Cheesman, N. Munksgaard, H. Stuart-Williams and G.D. Farquhar. 2016. Leaf vein fraction influences the Péclet effect and ^{18}O enrichment in leaf water. Plant Cell and Environment. 39:2414-2427.

Kahmen, A., K. Simonin, K. Tu, G.R. Goldsmith and T.E. Dawson. 2009. The influence of species and growing conditions on the 18-O enrichment of leaf water and its impact on 'effective path length'. New Phytologist. 184:619-630.

Kahmen, A., K. Simonin, K.P. Tu, A. Merchant, A. Callister, R. Siegwolf, T.E. Dawson and S.K. Arndt. 2008. Effects of environmental parameters, leaf physiological properties and leaf water relations on leaf water $\delta^{18}O$ enrichment in different Eucalyptus species. Plant, Cell & Environment. 31:738-751.

Labuhn, I., V. Daux, O. Girardclos, M. Stievenard, M. Pierre and V. Masson-Delmotte. 2016. French summer droughts since 1326 CE: a reconstruction based on tree ring cellulose $\delta^{18}O$. Climate of the Past. 12:1101-1117.

Laumer, W., L. Andreu, G. Helle, G.H. Schleser, T. Wieloch and H. Wissel. 2009. A novel approach for the homogenization of cellulose to use micro-amounts for stable isotope analyses. Rapid Commun Mass Spectrom. 23:1934-40.

Leavitt, S.W. and S.R. Danzer. 1993. Method for batch processing small wood samples to holocellulose for stable-carbon isotope analysis. Analytical Chemistry. 65:87-89.

Lehmann, M.M., B. Gamarra, A. Kahmen, R.T.W. Siegwolf and M. Saurer. 2017. Oxygen isotope fractionations across individual leaf carbohydrates in grass and tree species. Plant, Cell & Environment. 40:1658-1670.

Liang, J., J.S. Wright, X.W. Cui, L. Sternberg, W.X. Gan and G.H. Lin. 2018. Leaf anatomical traits determine the O-18 enrichment of leaf water in coastal halophytes. Plant Cell and Environment. 41:2744-2757.

Libby, L.M., L.J. Pandolfi, P.H. Payton, J. Marshall, B. Becker and V. Giertz-Sienbenlist. 1976. Isotopic tree thermometers. Nature. 261:284-288.

Masson-Delmotte, V., G. Raffalli-Delerce, P.A. Danis, P. Yiou, M. Stievenard, F. Guibal, O. Mestre, V. Bernard, H. Goosse, G. Hoffmann and J. Jouzel. 2005. Changes in European

precipitation seasonality and in drought frequencies revealed by a four-century-long tree-ring isotopic record from Brittany, western France. Climate Dynamics. 24:57-69.

McCarroll, D. and N.J. Loader. 2004. Stable isotopes in tree rings. Quaternary Science Reviews. 23:771-801.

McDowell, N.G., W.T. Pockman, C.D. Allen, D.D. Breshears, N. Cobb, T. Kolb, J. Plaut, J. Sperry, A. West, D.G. Williams and E.A. Yepez. 2008. Mechanisms of plant survival and mortality during drought: why do some plants survive while others succumb to drought? New Phytologist. 178:719-739.

Moreno-Gutiérrez, C., T.E. Dawson, E. Nicolás and J.I. Querejeta. 2012. Isotopes reveal contrasting water use strategies among coexisting plant species in a Mediterranean ecosystem. New Phytologist. 196:489-496.

Ogée, J., M.M. Barbour, L. Wingate, D. Bert, A. Bosc, M. Stievenard, C. Lambrot, M. Pierre, T. Bariac, D. Loustau and R.C. Dewar. 2009. A single-substrate model to interpret intra-annual stable isotope signals in tree-ring cellulose. Plant, Cell & Environment. 32:1071-1090.

Ogée, J., M. Cuntz, P. Peylin and T. Bariac. 2007. Non-steady-state, non-uniform transpiration rate and leaf anatomy effects on the progressive stable isotope enrichment of leaf water along monocot leaves. Plant, Cell & Environment. 30:367-387.

Pearson, M., M. Saarinen, L. Nummelin, J. Heiskanen, M. Roitto, T. Sarjala and J. Laine. 2013. Tolerance of peat-grown Scots pine seedlings to waterlogging and drought: Morphological, physiological, and metabolic responses to stress. Forest Ecology and Management. 307:43-53.

Pflug, E.E., R. Siegwolf, N. Buchmann, M. Dobbertin, T.M. Kuster, M.S. Günthardt-Goerg and M. Arend. 2015. Growth cessation uncouples isotopic signals in leaves and tree rings of drought-exposed oak trees. Tree Physiology. 35:1095-1105.

Poyatos, R., D. Aguadé, L. Galiano, M. Mencuccini and J. Martínez-Vilalta. 2013. Drought-induced defoliation and long periods of near-zero gas exchange play a key role in accentuating metabolic decline of Scots pine. New Phytologist. 200:388-401.

Rebetez, M. and M. Dobbertin. 2004. Climate change may already threaten Scots pine stands in the Swiss Alps. Theoretical and Applied Climatology. 79:1-9.

Rigling, A., C. Bigler, B. Eilmann, E. Feldmeyer-Christe, U. Gimmi, C. Ginzler, U. Graf, P. Mayer, G. Vacchiano, P. Weber, T. Wohlgemuth, R. Zweifel and M. Dobbertin. 2013. Driving factors of a vegetation shift from Scots pine to pubescent oak in dry Alpine forests. Global Change Biology. 19:229-240.

Rinne, K.T., N.J. Loader, V.R. Switsur and J.S. Waterhouse. 2013. 400-year May–August precipitation reconstruction for Southern England using oxygen isotopes in tree rings. Quaternary Science Reviews. 60:13-25.

Roden, J., A. Kahmen, N. Buchmann and R. Siegwolf. 2015. The enigma of effective path length for ^{18}O enrichment in leaf water of conifers. Plant, Cell & Environment. 38:2551-2565.

Roden, J.S. and J.R. Ehleringer. 1999. Observations of Hydrogen and Oxygen Isotopes in Leaf Water Confirm the Craig-Gordon Model under Wide-Ranging Environmental Conditions. Plant Physiology. 120:1165-1174.

Roden, J.S., J.A. Johnstone and T.E. Dawson. 2009. Intra-annual variation in the stable oxygen and carbon isotope ratios of cellulose in tree rings of coast redwood (*Sequoia sempervirens*). The Holocene. 19:189-197.

Roden, J.S., G. Lin and J.R. Ehleringer. 2000. A mechanistic model for interpretation of hydrogen and oxygen isotope ratios in tree-ring cellulose. Geochimica et Cosmochimica Acta. 64:21-35.

Rowland, L., A.C.L. da Costa, D.R. Galbraith, R.S. Oliveira, O.J. Binks, A.A.R. Oliveira, A.M. Pullen, C.E. Doughty, D.B. Metcalfe, S.S. Vasconcelos, L.V. Ferreira, Y. Malhi, J. Grace, M.

878 Mencuccini and P. Meir. 2015. Death from drought in tropical forests is triggered by
879 hydraulics not carbon starvation. Nature. 528:119-122.
880 Salmon, Y., J.M. Torres-Ruiz, R. Poyatos, J. Martinez-Vilalta, P. Meir, H. Cochard and M.
881 Mencuccini. 2015. Balancing the risks of hydraulic failure and carbon starvation: a twig
882 scale analysis in declining Scots pine. Plant, Cell & Environment. 38:2575-2588.
883 Sargeant, C.I. and M.B. Singer. 2016. Sub-annual variability in historical water source use by
884 Mediterranean riparian trees. Ecohydrology. 9:1328-1345.
885 Sarris, D., R. Siegwolf and C. Körner. 2013. Inter- and intra-annual stable carbon and oxygen
886 isotope signals in response to drought in Mediterranean pines. Agricultural and Forest
887 Meteorology. 168:59-68.
888 Saurer, M., K. Aellen and R. Siegwolf. 1997. Correlating $\delta^{13}C$ and $\delta^{18}O$ in cellulose of trees. Plant
889 Cell and Environment. 20:1543-1550.
890 Saurer, M., A.V. Kirdyanov, A.S. Prokushkin, K.T. Rinne and R.T.W. Siegwolf. 2016. The impact of
891 an inverse climate–isotope relationship in soil water on the oxygen-isotope composition
892 of Larix gmelinii in Siberia. New Phytologist. 209:955-964.
893 Saurer, M., A. Kress, M. Leuenberger, K.T. Rinne, K.S. Treydte and R.T.W. Siegwolf. 2012.
894 Influence of atmospheric circulation patterns on the oxygen isotope ratio of tree rings
895 in the Alpine region. Journal of Geophysical Research: Atmospheres. 117:2156-2202.
896 Scheidegger, Y., M. Saurer, M. Bahn and R. Siegwolf. 2000. Linking stable oxygen and carbon
897 isotopes with stomatal conductance and photosynthetic capacity: a conceptual model.
898 Oecologia. 125:350-357.
899 Song, X., G.D. Farquhar, A. Gessler and M.M. Barbour. 2014. Turnover time of the non-structural
900 carbohydrate pool influences $\delta^{18}O$ of leaf cellulose. Plant Cell and Environment.
901 37:2500-2507.
902 Song, X., K.E. Loucos, K.A. Simonin, G.D. Farquhar and M.M. Barbour. 2015. Measurements of
903 transpiration isotopologues and leaf water to assess enrichment models in cotton. New
904 Phytologist. 206:637-646.
905 Song, X.I.N., M.M. Barbour, G.D. Farquhar, D.R. Vann and B.R. Helliker. 2013. Transpiration rate
906 relates to within- and across-species variations in effective path length in a leaf water
907 model of oxygen isotope enrichment. Plant, Cell & Environment. 36:1338-1351.
908 Sternberg, L. 2009. Oxygen stable isotope ratios of tree-ring cellulose: the next phase of
909 understanding. New Phytologist. 181:553-62.
910 Sternberg, L., M.J. Deniro and R.A. Savidge. 1986. Oxygen Isotope Exchange between
911 Metabolites and Water during Biochemical Reactions Leading to Cellulose Synthesis.
912 Plant Physiology. 82:423-427.
913 Timofeeva, G., K. Treydte, H. Bugmann, A. Rigling, M. Schaub, R. Siegwolf and M. Saurer. 2017.
914 Long-term effects of drought on tree-ring growth and carbon isotope variability in Scots
915 pine in a dry environment. Tree Physiol:1-14.
916 Treydte, K., S. Boda, E. Graf Pannatier, P. Fonti, D. Frank, B. Ullrich, M. Saurer, R. Siegwolf, G.
917 Battipaglia, W. Werner and A. Gessler. 2014. Seasonal transfer of oxygen isotopes from
918 precipitation and soil to the tree ring: source water versus needle water enrichment.
919 New Phytologist. 202:772-783.
920 Treydte, K., D. Frank, J. Esper, L. Andreu, Z. Bednarz, F. Berninger, T. Boettger, C.M. D'Alessandro,
921 N. Etien, M. Filot, M. Grabner, M.T. Guillemin, E. Gutierrez, M. Haupt, G. Helle, E.
922 Hilasvuori, H. Jungner, M. Kalela-Brundin, M. Krapiec, M. Leuenberger, N.J. Loader, V.
923 Masson-Delmotte, A. Pazdur, S. Pawelczyk, M. Pierre, O. Planells, R. Pukiene, C.E.
924 Reynolds-Henne, K.T. Rinne, A. Saracino, M. Saurer, E. Sonninen, M. Stievenard, V.R.
925 Switsur, M. Szczepanek, E. Szychowska-Krapiec, L. Todaro, J.S. Waterhouse, M. Weigl
926 and G.H. Schleser. 2007. Signal strength and climate calibration of a European tree-ring
927 isotope network. Geophysical Research Letters. 34:L24302.

928 Treydte, K.S., G.H. Schleser, G. Helle, D.C. Frank, M. Winiger, G.H. Haug and J. Esper. 2006. The
929 twentieth century was the wettest period in northern Pakistan over the past
930 millennium. Nature. 440:1179-1182.
931 Ueta, A., A. Sugimoto, Y. Iijima, H. Yabuki, T.C. Maximov, T.A. Velivetskaya and A.V. Ignatiev.
932 2013. Factors controlling diurnal variation in the isotopic composition of atmospheric
933 water vapour observed in the taiga, eastern Siberia. Hydrological Processes. 27:2295-
934 2305.
935 Volkmann, T.H.M., K. Haberer, A. Gessler and M. Weiler. 2016. High-resolution isotope
936 measurements resolve rapid ecohydrological dynamics at the soil-plant interface. New
937 Phytologist. 210:839-849.
938 Waterhouse, J.S., V.R. Switsur, A.C. Barker, A.H.C. Carter and I. Robertson. 2002. Oxygen and
939 hydrogen isotope ratios in tree rings: how well do models predict observed values?
940 Earth and Planetary Science Letters. 201:421-430.
941 Weigt, R.B., S. Bräunlich, L. Zimmermann, M. Saurer, T.E.E. Grams, H.-P. Dietrich, R.T.W. Siegwolf
942 and P.S. Nikolova. 2015. Comparison of $\delta^{18}O$ and $\delta^{13}C$ values between tree-ring whole
943 wood and cellulose in five species growing under two different site conditions. Rapid
944 Communications in Mass Spectrometry. 29:2233-2244.
945 West, A.G., S.J. Patrickson and J.R. Ehleringer. 2006. Water extraction times for plant and soil
946 materials used in stable isotope analysis. Rapid Commun Mass Spectrom. 20:1317-21.
947 Yakir, D., M.J. DeNiro and J.R. Gat. 1990. Natural deuterium and oxygen-18 enrichment in leaf
948 water of cotton plants grown under wet and dry conditions: evidence for water
949 compartmentation and its dynamics. Plant, Cell & Environment. 13:49-56.
950 Zwieniecki, M.A., T.J. Brodribb and N.M. Holbrook. 2007. Hydraulic design of leaves: insights
951 from rehydration kinetics. Plant Cell and Environment. 30:910-921.

952

Table 1. Transpiration rates for the period of 2013-2014. Numbers are mean values of four trees ± standard deviation. NA – not available (only one tree measured).

Date	Transpiration rate (mmol m^{-2} s^{-1})	
	Drought-stressed	Irrigated
18.06. 2013	0.35 ± 0.08	0.36 ± 0.17
06.05.2014	0.22 ± 0.07	1.01 ± NA
03.06.2014	0.12 ± 0.05	0.21 ± 0.05
2013-2014	0.24 ± 0.12	0.43 ± 0.34

Table 2. Needle length data determined during summer 2013 and 2014. Numbers are mean values (± standard deviation) of 10 drought-stressed and 12 irrigated trees.

Date	Needle length (mm)	
	Drought-stressed	Irrigated
2013	38.77 ± 7.61	48.24 ± 7.27
2014	30.57 ± 8.57	40.38 ± 8.45
2013-2014	34.67 ± 8.94	44.31 ± 8.69

Table 3. Average cross-sectional areas of different tissues (±standard deviation) for both treatments and two needle generations as well as the proportion of isotopically non-enriched tissue. Non-enriched is defined as the sum of endodermis, xylem, phloem and transfusion tissues.

Treat-ment	needle gener-ation	needle (mm^2)	Epider-mis + hypoder-mis (mm^2)	resin ducts (mm^2)	meso-phyll (mm^2)	Endo-dermis (mm^2)	Transfu-sion tissues (mm^2)	Phloem (mm^2)	Xylem (mm^2)	=non-enri-ched/total
Drought -stressed	2013	0.868 ±0.137	0.128 ±0.016	0.091 ±0.017	0.415 ±0.067	0.040 ±0.007	0.166 ±0.036	0.020 ±0.004	0.008 ±0.002	0.269 ±0.015
Irrigated	2013	0.900 ±0.187	0.132 ±0.019	0.097 ±0.026	0.417 ±0.095	0.040 ±0.006	0.180 ±0.042	0.024 ±0.007	0.012 ±0.004	0.283 ±0.013
Drought -stressed	2014	0.694 ±0.131	0.110 ±0.017	0.074 ±0.015	0.322 ±0.065	0.031 ±0.005	0.138 ±0.031	0.013 ±0.003	0.006 ±0.002	0.271 ±0.014
Irrigated	2014	0.810 ±0.211	0.121 ±0.023	0.088 ±0.026	0.373 ±0.106	0.036 ±0.007	0.166 ±0.049	0.016 ±0.005	0.010 ±0.003	0.281 ±0.012

Table 4. List of parameters and leaf water model results calculated as average of all sampling days during the growing seasons (omitting Oct-Feb data). The equilibrium fractionation $\varepsilon+$ is calculated according to Eq. 3, the diffusivity D according to Cuntz et al. (2007), the path length L obtained through optimization (see text for details), the Péclet number $\wp$ calculated with Eq. 4, the proportion of isotopically non-enriched tissue φ determined from anatomical measurements. $\Delta^{18}O_N$ is the measured difference between $\delta^{18}O_N$ and $\delta^{18}O_{soil\ 20\ cm}$, $\Delta^{18}O_{CG}$ calculated according to Eq. 2 and $\Delta^{18}O_{full\ model}$ according to Eq. 7.

Parameter	drought-stressed	irrigated
$\varepsilon+$ (‰)	8.94	8.82
ε_k (‰)	28	28
D ($m^2 s^{-1}$)	2.53e-09	2.62e-09
L (m)	0.32	0.05
E (mmol m^{-2} s^{-1})	0.28	0.55
EL (mmol m^{-1} s^{-1})	0.09	0.03
$\wp$	0.63	0.19
φ	0.27	0.28
$\delta^{18}O_{soil\ 20cm}$ (‰)	-6.84	-9.43
$\delta^{18}O_N$ (‰)	5.99	6.90
$\Delta^{18}O_N$ (‰)	12.83	16.33
$\Delta^{18}O_{CG}$ (‰)	23.31	24.76
$\Delta^{18}O_{full\ model}$ (‰)	12.62	16.15

Figure captions

Fig. 1. Seasonal variations in $\delta^{18}O$ of needle water (a), soil water at 0-10 cm (b) and at 10-20 cm (c) shown for drought-stressed and ambient plots. Isotope values of channel water used for irrigation are displayed as stars (b, c).

Fig. 2. Seasonal changes in needle water ^{18}O enrichment ($\Delta^{18}O$) calculated as difference between needle water $\delta^{18}O$ and soil water at 10-20 cm.

Fig. 3. Relationship between measured and predicted needle water ^{18}O enrichment using the basic Craig-Gordon model (Eq. 2, a) and the full model with the combined Péclet- and two-pool correction (Eq. 7, b). Regression lines and equations are also indicated. The dashed lines show 95% confidence intervals.

Fig. 4. Tree-ring $\delta^{18}O$ chronologies of living and now-dead trees (a) and their differences (b). The dashed lines indicate the mean of the differences between dead and living for 1900-1959 and 1960-2005, respectively. Note: the chronology of the dead trees covers the period 1900-2005.

Fig. 5. Pearson's correlation coefficients between $\delta^{18}O$ chronologies and climate variables (T – mean temperature, P – precipitation amount, SPEI – standardized precipitation-evapotranspiration index (3m = 3 months, 6m = 6 months), RH – relative humidity, VPD – vapour pressure deficit) for the period of 1960-2003 for spring (March-May; a) and summer (June to August; b). White bars refer to living trees and black bars to dead trees. Significant correlations are marked by * ($P < 0.05$) and ** ($P < 0.01$).

Fig. 6. Time series of observed (living/now-dead) and predicted tree-ring cellulose $\delta^{18}O$ values using the basic and the full CG-model with the Péclet and two-pool corrections (Eq. 8). The effect of varying L in the full model is also shown.

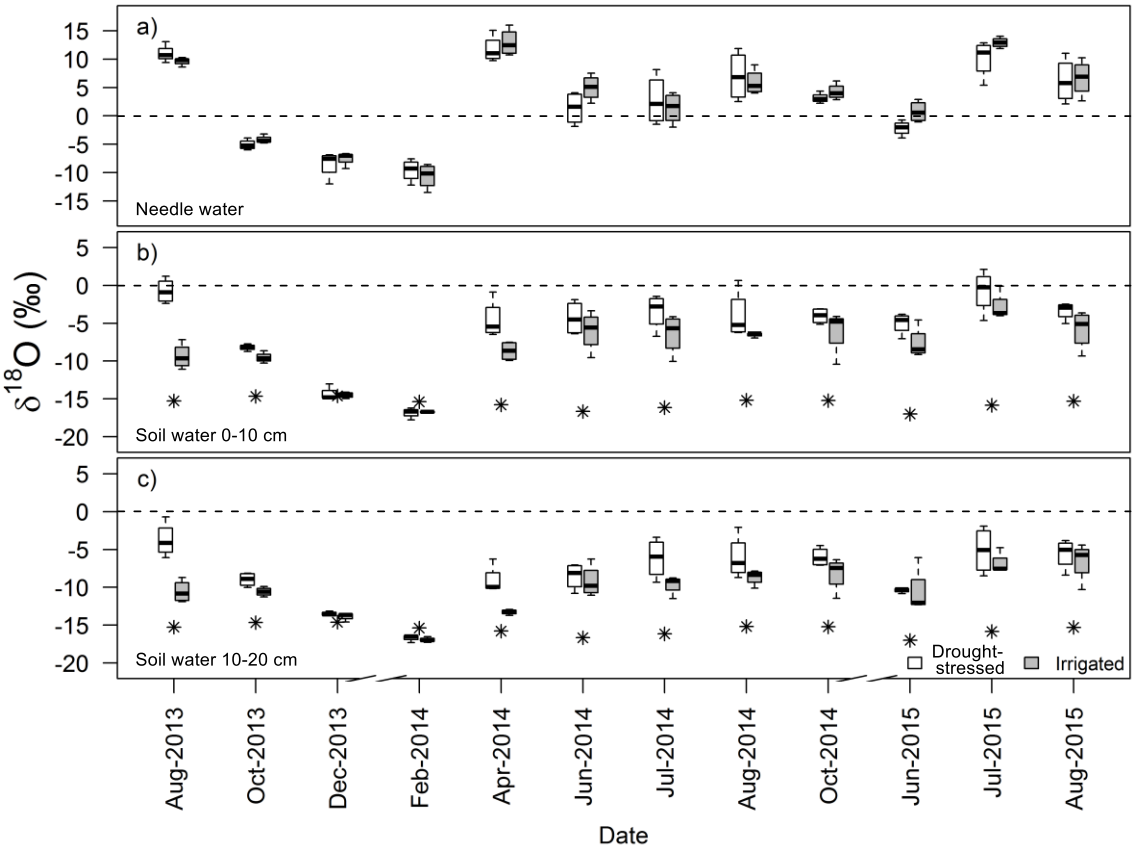
a)
Needle water
b)
Soil water 0-10 cm
c)
Soil water 10-20 cm
δ18O (‰)
Drought-stressed
Irrigated
Aug-2013
Oct-2013
Dec-2013
Feb-2014
Apr-2014
Jun-2014
Jul-2014
Aug-2014
Oct-2014
Jun-2015
Jul-2015
Aug-2015
Date

Figure 1.

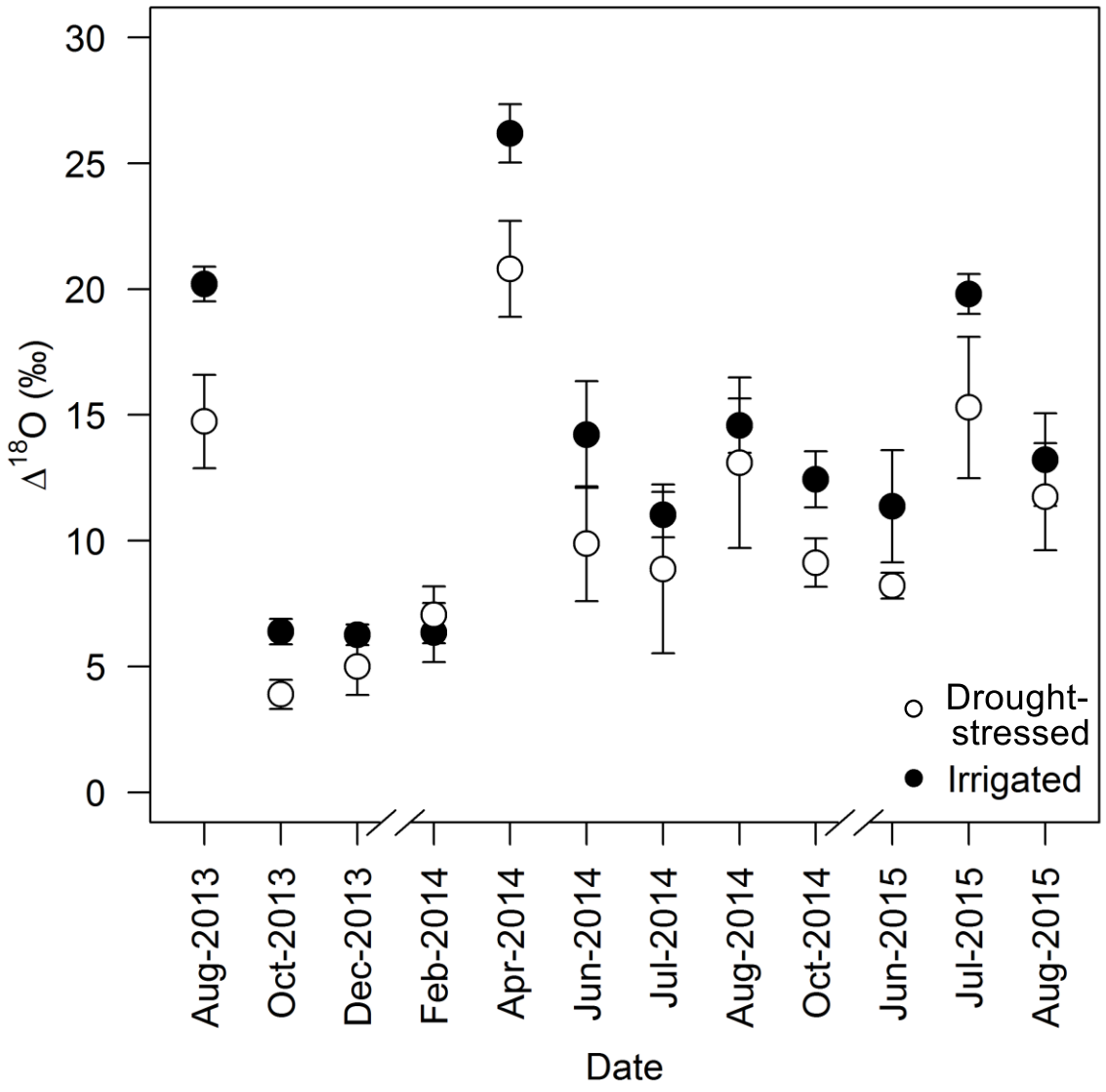
30
25
20
15
10
5
0
$\Delta^{18}O$ (‰)
Drought-stressed
Irrigated
Aug-2013
Oct-2013
Dec-2013
Feb-2014
Apr-2014
Jun-2014
Jul-2014
Aug-2014
Oct-2014
Jun-2015
Jul-2015
Aug-2015
Date

Figure 2.

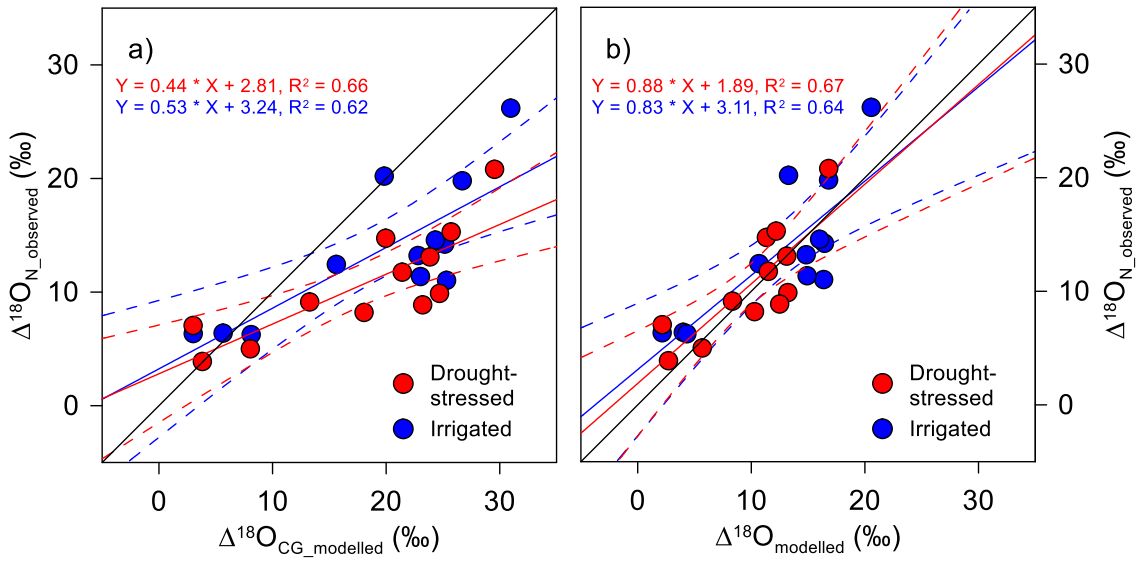
a)
Y = 0.44 * X + 2.81, R² = 0.66
Y = 0.53 * X + 3.24, R² = 0.62
Drought-stressed
Irrigated
Δ18O_N_observed (‰)
Δ18O_CG_modelled (‰)
b)
Y = 0.88 * X + 1.89, R² = 0.67
Y = 0.83 * X + 3.11, R² = 0.64
Drought-stressed
Irrigated
Δ18O_N_observed (‰)
Δ18O_modelled (‰)

Figure 3.

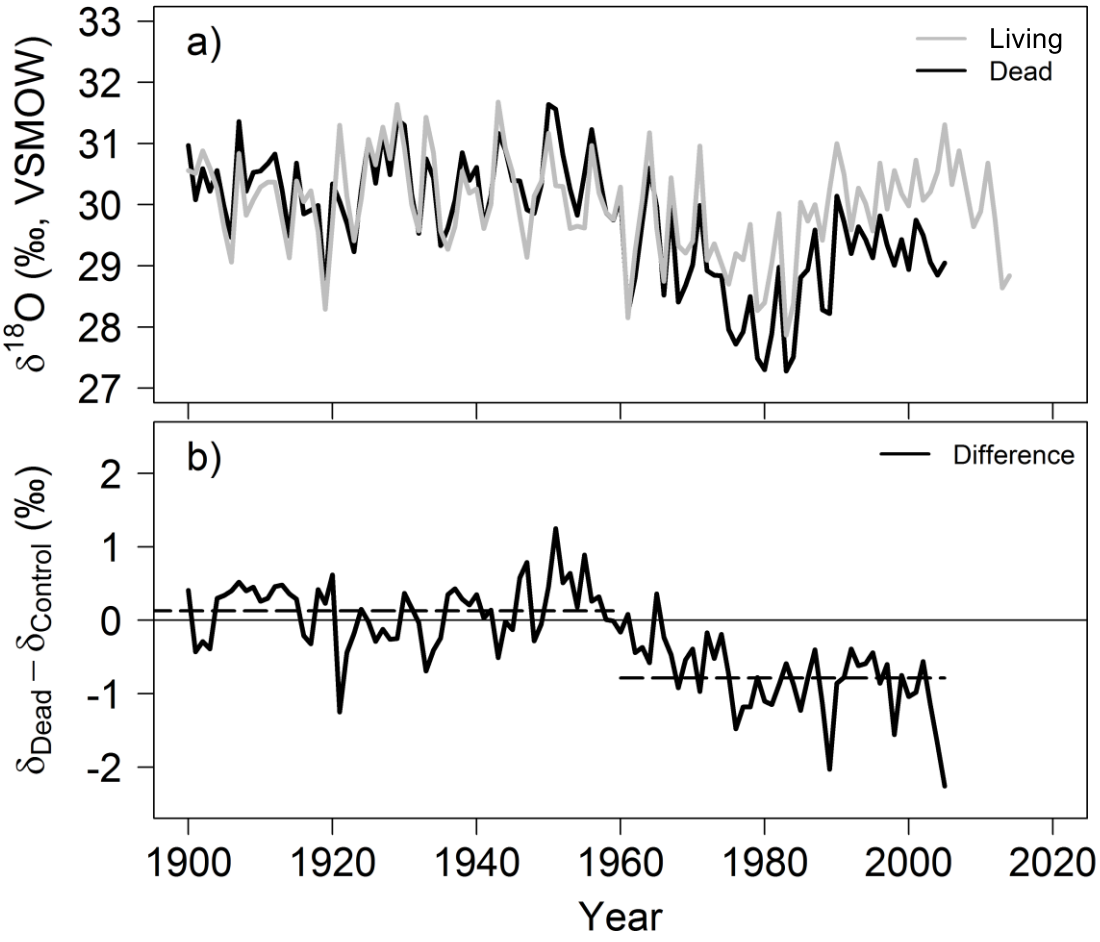
a)
Living
Dead
$\delta^{18}O$ (‰, VSMOW)
33
32
31
30
29
28
27
b)
Difference
$\delta_{Dead} - \delta_{Control}$ (‰)
2
1
0
-1
-2
1900
1920
1940
1960
1980
2000
2020
Year

Figure 4.

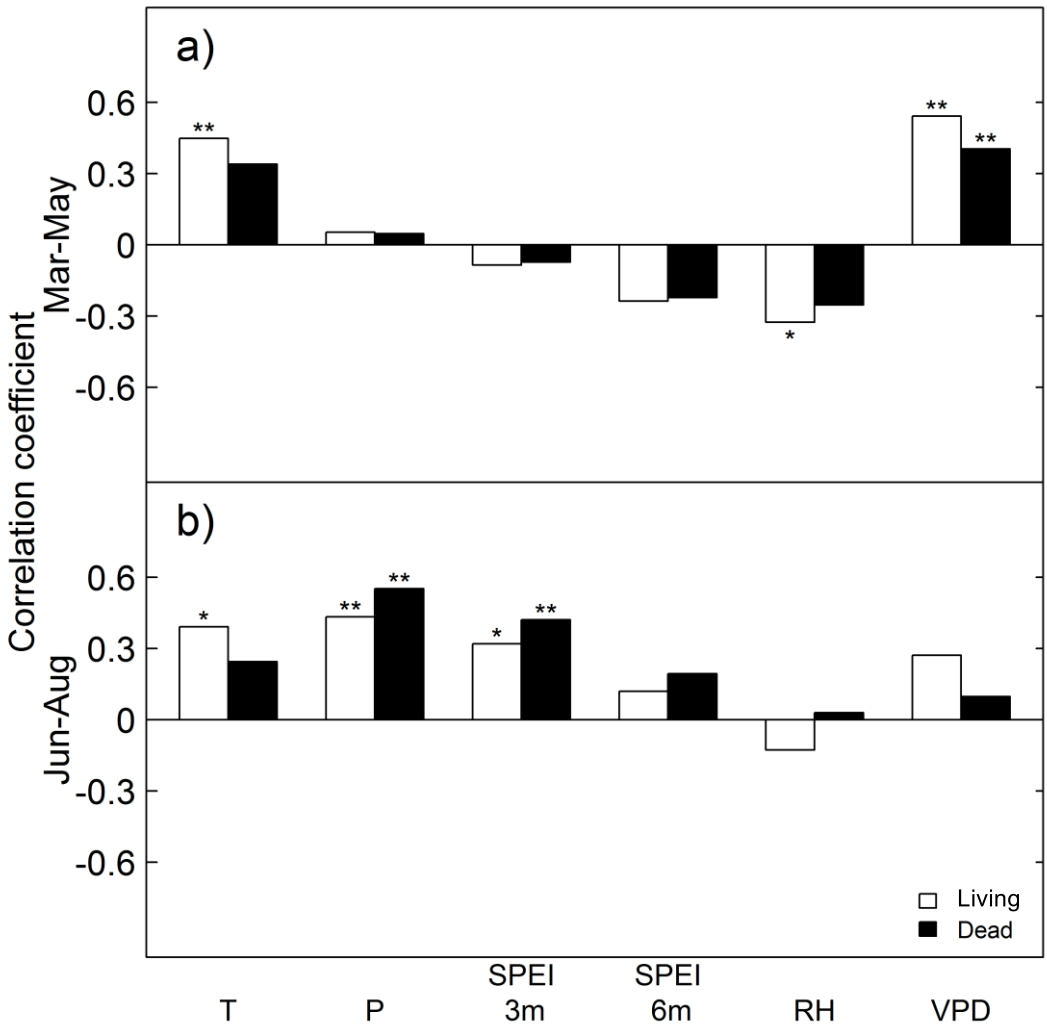
a)
b)
Correlation coefficient
Mar-May
Jun-Aug
0.6
0.3
0
-0.3
-0.6
Living
Dead
T
P
SPEI 3m
SPEI 6m
RH
VPD

Figure 5.

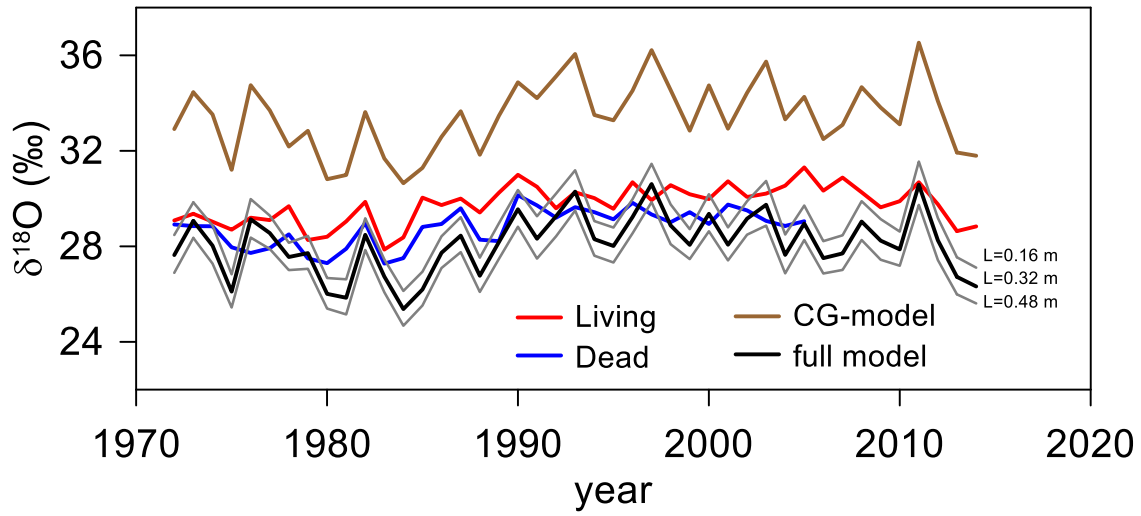
36
32
28
24
δ18O (‰)
1970
1980
1990
2000
2010
2020
year
Living
Dead
CG-model
full model
L=0.16 m
L=0.32 m
L=0.48 m

Figure 6.